Int. J. Electrochem. Sci., 7 **(2012)** 11596 - 11608

International Journal of
ELECTROCHEMICAL
SCIENCE
www.electrochemsci.org

Evidence for the Formation of a Copolymer by Simultaneous Electropolymerization of p-Tetraaminophenyl Porphyrin Cobalt (II)) and *o*-Phenylenediamine on Glassy Carbon

Roxana Arce[1,*], *Rodrigo del Río*[2], *Domingo Ruiz-León*[1], *Jorge Velez*[1], *Mauricio Isaacs*[2],
María A. del Valle[2] *and María J. Aguirre*[1]

[1] Departamento de Química de los Materiales, Facultad de Química y Biología, Universidad de Santiago de Chile, Alameda 3363, Estación Central, Santiago, Chile
[2] Departamento de Química Inorgánica, Facultad de Química, Pontificia Universidad Católica de Chile, Av. Vicuña Mackenna 4860, Macul, Santiago, Chile.
[*]E-mail: arce.roxana@gmail.com

Received: 22 August 2012 / *Accepted:* 9 October 2012 / *Published:* 1 November 2012

There is relatively little research about the simultaneous electropolymerization of porphyrins and aniline derivatives in aqueous media. Normally, the copolymerization studies are focused in the polymerization of two conducting monomers without a redox metal center. It is interesting to study a probable synergic effect among very different species as metalled porphyrins and aniline derivatives. The synergic effect of a real co-polymerization would affect the electrochemical and mechanical properties. Electropolymerization of *p*-tetra-aminophenyl porphyrin of cobalt (II), polyCoTAPP, generates thin and fragile films that "crystallize" on some electrode surfaces in aqueous media. They are very electroactive but unstable in aqueous media. On the other hand, the electropolymerization of *o*-phenylenediamine, P*o*PD, generates stable and thick films with electroactivity to some reduction reactions and without redox response in the positive range between *ca*. 0.0 and 0.8V *vs* Ag/AgCl. In this research we electropolymerize both species dissolved in acid aqueous media obtaining a new film that has different properties compared to the homopolymers. Raman and XPS studies demonstrate the copolymerization and the synergic effect on the growing of the film.

Keywords: conducting polymer; poly(*o*-phenylenediamine); poly(*p*-tetra-aminophenyl) porphyrin of cobalt (II); copolymer

1. INTRODUCTION

Conducting polymers have become very popular in the field of materials science due to their promising and novel electrical properties such as energy storage devices [1,2], gas sensors [3,4], EMI shielding [5,6], electrostatic charge dissipation [7,8], OLED and flexible display devices [9,10], anticorrosive metals [11,12], and electrochromic materials [13,14]. Among all conducting polymers, P*o*PD [15] has a special representation due to easy synthesis being obtained as a layer of self-limiting thickness on different conducting substrates via anodic electropolymerization. P*o*PD layers have been well characterized by electrochemical, quarz crystal microbalance, radiotracer, STM and different spectroscopic techniques. These layers are permselectivite and stable [15].

Synthesis of P*o*PD is usually carried out electrochemically in acid, neutral and alkaline solutions and is very stable in both aqueous solutions and air [16]. The ease of dissolution of P*o*PD in organic solvents such as dimethyl sulfoxide makes it one of the so-called soluble electroactive polymers [17-18]. During the electropolymerization process, polymer film is deposited on the electrode surface and the formation of soluble oligomers might occur. The local concentration of the oligomers near the electrode surface might be very high, depending on the solubility and the diffusivity of the oligomers. The polymer films formed might be very porous [16].

Another type of conducting polymer is a redox polymer. Polymerized porphyrins and metalloporphyrins can be used to coat electrodes showing interesting features as analytical sensors because they can electrocatalyze many charge transfer processes increasing the sensitivity and selectivity of the electrode [19-25]. In particular, amino-substituted porphyrins can be electropolymerized to afford surface-modified electrodes aimed at preparing sensors [26-28] such as polyCoTAPP. Synthesis of polyCoTAPP is usually carried out electrochemically in organic solvents where the deposit is stable and reproducible [29]. Rarely is carried out in aqueous solution but in our group we have experience in polymerization and copolymerization of metaloporphyrins in aqueous media [30]. In all cases, electropolymerization occurs by the oxidation of the amino groups and the subsequent *para* coupling, forming films on a conductive substrate [31-32]. Characteristics of electrochemical copolymerization are highly dependent on the synthesis conditions of the electropolymerization of monomers [33-37].

The formation of poly(CoTAPP-co-*o*PD) copolymer in acid solution is due to the insolubility of *o*PD in organic solvents. Taking into account that polyCoTAPP forms unstable and fragile films in aqueous media [38], copolymerization between CoTAPP and *o*PD molecules could improve the electrical properties and the stability of this new material because *o*PD forms conductive coatings, thick and stable [16].

This research is focused in obtaining evidence of the formation of a real copolymer and not a mixture or composite of oligomers formed by only a molecule (homo-oligomers). On the other hand, our aim is to observe synergic effects on the polymerization or in the electrocatalytic behavior. We report here the results obtained in the synthesis and characterization of homopolymers and copolymers of CoTAPP y *o*PD. Electrochemical and spectroscopical techniques were used to study the electropolymerization processes of this copolymer in sulfuric acid solution as supporting electrolyte. The reduction of dioxygen was used as a test reaction to measure electroactivity. In literature, there is a report where it is shown a major electrocatalytic activity when it is used a copolymer of an iron porphyrin and aniline [30]. We tried to obtain quantitative and qualitative data for obtaining a better understanding of the copolymerization processes involved.

2. EXPERIMENTAL PART

o-phenylenediamine (Merck) and 5,10,15,20-tetraaminophenyl-porphyrin cobalt (II) (Organix) were used as received. All solutions used contained 0.1 mol·L^{-1} sulfuric acid.

All the experiments reported were carried out in a conventional three-compartment cell. A glassy carbon disc (GC) (geometrical area 0.07 cm^2) and Ag/AgCl were used as working and reference electrodes, respectively. The reference electrode was placed in a compartment separated from the working electrode by a Luggin capillary. The counter electrode was a Pt wire of large area, separated from the working electrode by a fine glass frit. Before each experiment the working electrode was polished with alumina slurry (particle size 0.3 µm) on soft leather and afterward washed with deionized water. Before all the experiments, solutions were purged with high-purity nitrogen atmosphere. This atmosphere was maintained over the solution during measurements, except when O_2 is bubbled (99.995 % AGA).

Electrochemical polymerization was carried out from solutions containing 0.1 mol·L^{-1} monomer of *o*PD; 0.1 mmol·L^{-1} monomer of CoTAPP and 0.1 mol·L^{-1} background electrolyte. P*o*PD was obtained by applying a potential between 0.0 and 0.8 V versus Ag/AgCl electrode at 0.05 V·s^{-1} and poly(CoTAPP) was prepared by applying a potential between -0.6 and 1.0 V versus Ag/AgCl electrode at 0.05 V·s^{-1}.

Electrochemical copolymerization was carried out from solutions containing 0.1 mol·L^{-1} of *o*PD and 0.1 mmol·L^{-1} of CoTAPP by feeding 1:1 v/v of each solution. The resultant solution was used to cycle the electrode between -0.6 and 1.0 V versus Ag/AgCl at 0.05 V·s^{-1}.

For impedance experiments, the frequency response analysis of the polymers was measured using a CHI potentiostiat (model 604C) over a frequency range from 0.1 mHz to 10 kHz. The impedance was measured at 10 discrete frequencies per decade in each scan with amplitude of 5 mV. This electrochemical technique was used to determine qualitatively electrical properties of the materials obtained. Impedance curves were obtained for the potentials: 0.0; 0.2; 0.4; 06 and 0.8 V. As pre-treatment, before each measurement, the electrode was polarized at a given potential for 1600 s. The current vs time tests when applying the potential showed that 1600 s were enough to reach cero current, that is to say, an equilibrium state. The potentials that were applied were not arbitrary. They were selected according the redox processes involved for each of the polymers. The adjustment was performed by using a very simple equivalent circuit and using the electrochemical impedance computer program ZWiew, in which the data were simulated and interpreted according to this circuit. A detail physical interpretation of this circuit was not made because of the enormous complexity of the real circuit. The equivalent circuit which was used was R_s-R_{pol}/CPE (C), where R_s corresponds to the serial resistances, R to the parallel resistances and CPE is an element of constant phase. This circuit, as said before, must contain at least one capacitor that represents the electrical double layer, a resistance which corresponds to the ohmic solution resistance and impedance which represents a faradaic process. The equivalent circuit consists of a resistance (ohmic, solution) in series with an element of constant phase (solution electrode interphase) which is in parallel with a resistance (resistance to the polymer charge transference) in parallel with other constant phase element (solution polymer interphase).

SEM measurements were made with a scanning electron microscope JEOL (model 6400) equipped with an energy dispersive detector OXFORD LINK ISIS. These experiments were used to determine the composition of the films and for the observation of their surface and morphology.

Micro-Raman spectroscopy studies were performed using a spectrometer Raman LabRam (model 010). This spectroscopy study was made possible to verify the formation of a copolymer between *o*PD and CoTAPP.

3. RESULTS AND DISCUSSIONS

3.1. Electropolymerization of homo and copolymers

Figure 1 shows the structure of the two monomers used in this study. Figure 2 shows the profiles of the voltammetric response of the electropolymerization of the homo and the copolymer on a glassy carbon. Results showed here correspond to the best results when varying relative concentrations of each monomer in the solution and optimizing the limits of potential and the number of potentiodynamic cycles. Figure 2A shows the electropolymerization of P*o*PD where an irreversible oxidation wave corresponding to the oxidation of amino groups appears (peak II). It has been reported that *o*PD oxidation produces the phenazine, which as shown in Diagram 1 gives rise to the ladder polymer [39-42]. Figure 2B corresponds to the electropolymerization of polyCoTAPP where a redox reversible couple attributed to CoIII/II is observed at *ca*. 0.5 V. Figure 2C corresponds to the copolymerization of poly(CoTAPP-co-*o*PD). In each Figure the irreversible oxidation wave corresponding to the oxidation of the amino groups (II) appears at positive limits. It is interesting to observe the difference in the intensity of the current that is directly proportional to the amount of active polymer deposited on the surface of the electrode. It is clear that the polyCoTAPP is very thin compared to the others. In C, peak I corresponds to the phenacine/phenacile redox couple $P^{\bullet+}/P$ [43] (see Diagram 1) of the *o*PD.

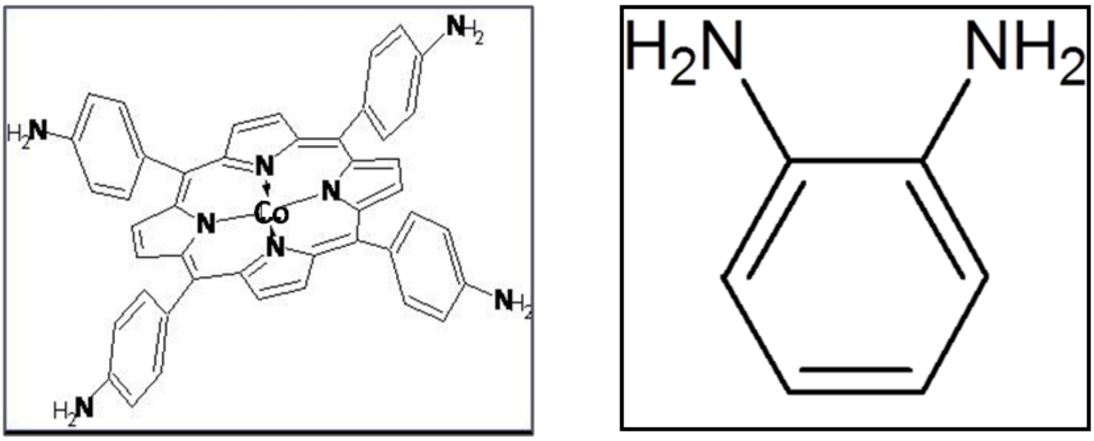

Figure 1. Structural formula of *p*-tetra-aminofenilporphyrin of cobalt (II) CoTAPP (right). Structure of *o*-phenylenediamine *o*PD (left).

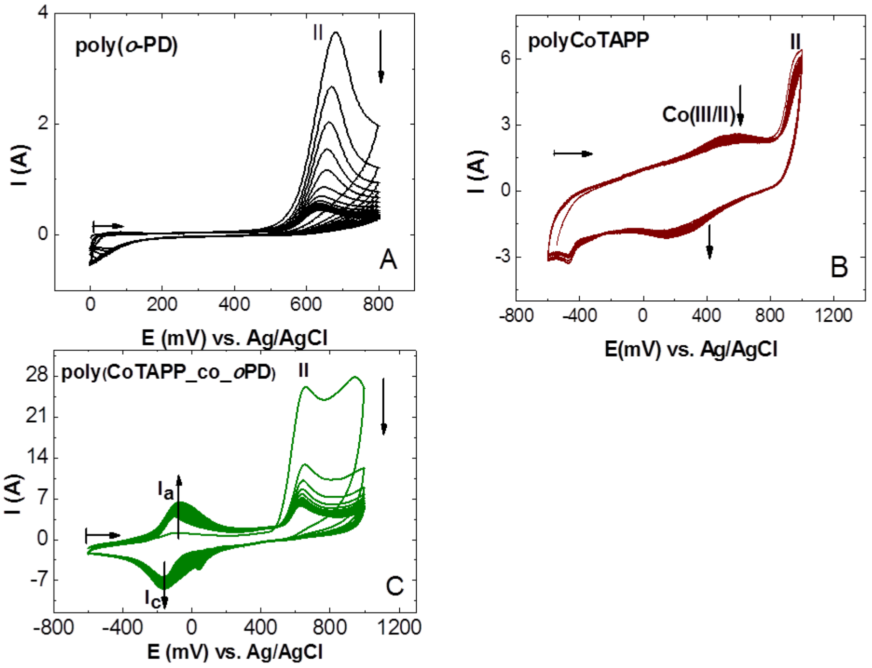

Figure 2. Voltammetric profiles obtained during the electropolymerization of poly (*o*PD) (A), poly (CoTAPP) (B), and poly (*o*PD-co-CoTAPP) (C) on glassy carbon in 0.1mol·L^{-1} H_2SO_4. v = 50 mV·s^{-1}. Cycles 1 to 15.

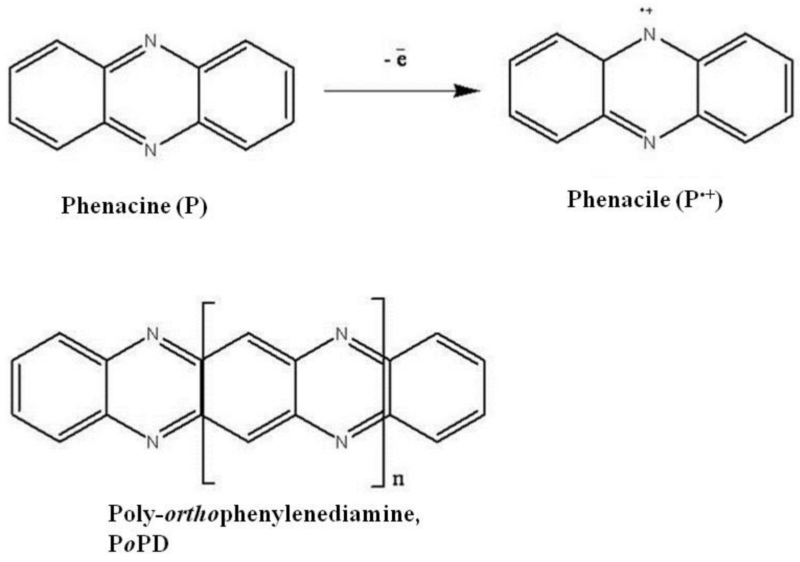

Diagram 1. (Top) Chemical structure of the redox couple of P*o*PD. (Bottom) The structure of the polymer formed by *o*PD.

Figure 3 shows the superposition of the response of the ultimate redox cycle (cycle 15) of both homopolymers and the copolymer. It is interesting that the charge of the copolymer is larger than the sum of the charge of each polymer. Deconvolution of the anodic peaks corresponding to the $P^{\bullet+}/P$ couple and CoII/I couple indicates a charge relation of 4:1 between those peaks indicating that the copolymer contains 4 *o*PD for each CoTAPP.

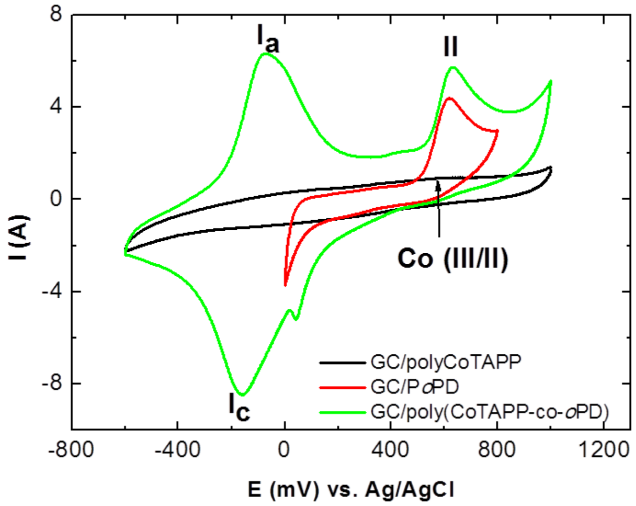

Figure 3. Comparative voltammetric profiles obtained during the electropolymerization of polyCoTAPP, PoPD and the copolymer on glassy carbon electrode in 0.1mol·L^{-1} H_2SO_4. v = 50 mV·s^{-1}. Cycle 15.

On the other hand, the electrocatalytic activity toward the reduction of oxygen (Fig. 4) shows that poly(CoTAPP-co-*o*PD) presents better results compared to the other homopolymers. There is a shift in the foot of the current wave to more positive potentials (*ca*. 40mV) for the copolymer compared to the P*o*PD. For the P*o*PD, the reduction wave appears at potentials slightly shifted to negative potentials compared to the Ep of the cathodic peak $P^{\bullet+}/P$ (not shown). This peak that occurs at more positive potentials than the redox couple CoII/I shows that modified electrode is a better redox mediator for this reaction due to the fact of the potential required to transfer an electron. P*o*PD, shows a displacement of the foot of wave of approximately 560 mV in comparison with GC in presence of molecular oxygen and the reduction wave practically coincides with the redox couple $P/P^{\bullet+}$ in the absence of O_2. GC/polyCoTAPP shows good electrocalatylic activity, observing a displacement of the foot of the wave of approximately 200 mV toward less negative potentials in comparison to GC. Finally the copolymer shifts the potential 600mV more positive than glassy carbon.

Besides, the three systems of modified electrodes turned out to be stables after 10 successive potential cycles.

This first result shows a small synergic effect in the electrocatalytic activity of the copolymer compared to both homopolymers.

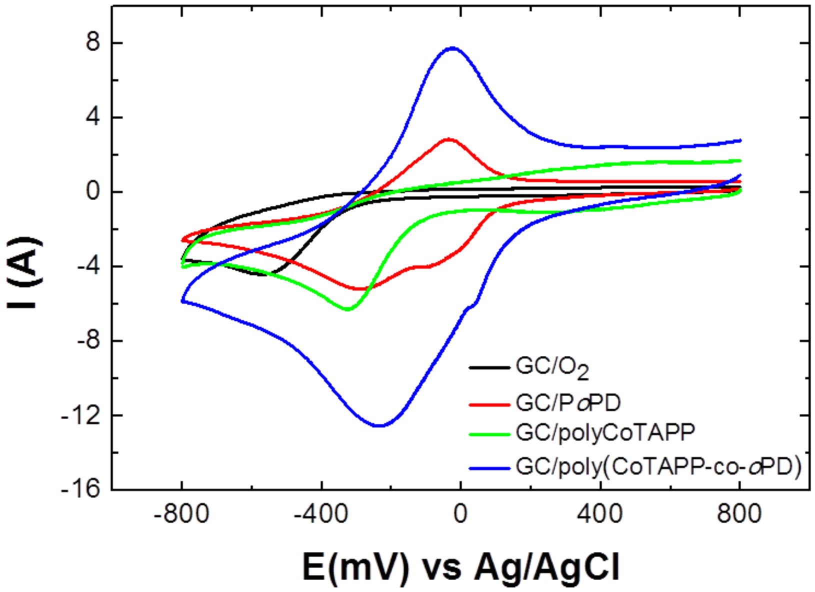

Figure 4. Profiles of comparative voltammetry of glassy carbon electrode modified with polyCoTAPP, P*o*PD and copolymer for the RRO v: 100 mV·s^{-1}. Cycle 1.

The impedance studies using the simple electric circuit model (see Fig. 5) shows how the copolymer has better electric response that both homopolymers. (see Tables 1).

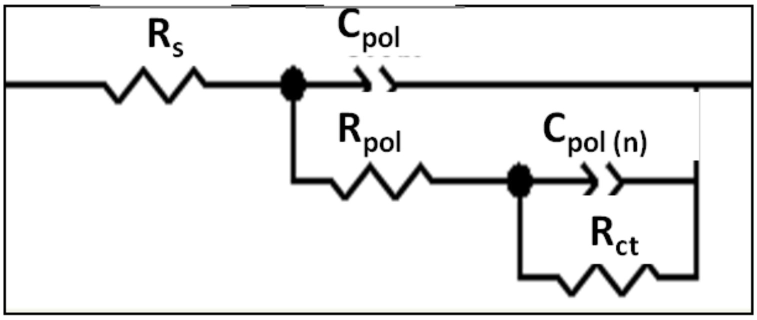

Figure 5. Equivalent circuit used in the analysis of electrochemical impedance data. R_s (strength solution) and C_{pol}, C_{pol} (n) (polymer solution interface and electrode solution interface, respectively) and R_{ct}, R_{pol} (resistance of the charge transfer of the polymer and of the double layer, respectively).

Table 1 shows the results for R_s, R_p y CPE, for the GC/P*o*PD, GC/polyCoTAPP and GC/poly(CoTAPP_co_*o*PD) electrodes at different potentials.

In Table 1 the results for the GC/P*o*PD electrode are shown, which presents “in serie” resistance ranging between 50 and 46 Ω, mainly attributed to the electrolyte resistance. The resistance of the R_{pol} polymer is around 20 kΩ, what means that this polymer is conductive for all the potential range and the capacity of the C_{pol} polymer (µF) is close to $1 \cdot 10^{-6}$ µF. The exponent of the frequency in the constant phase element, C_{pol} (n), of the order of 0.8. A 0.2 and 0.4 V, the values of R_{ct} are too high (of the order of $1 \cdot 10^{17}$ Ω) due to the fact that at those potentials there are no charge transference processes for this polymer. At 0.0 V a little lower charge transference resistance values are obtained, due to the fact that the potential is close to where the polymer redox process occurs. That is to say, the *o*PD polymer shows a R_{ct} of of $3.35 \cdot 10^{14}$ Ω to 0.0 V, which drastically changes with the increase in the potential by the presence of the faradaic reaction $P/P^{\bullet+}$ [44].

Table 1. Impedance parameters for the GC/P*o*PD, GC/polyCoTAPP and GC/poly(CoTAPP-co-*o*PD) electrodes.

P*o*PD					
Potential /V	R_s / Ω	C_{pol} / µF	C_{pol} / n	R_{pol} / kΩ	R_{ct} / Ω
0,0	50	0.7	0.8	17	$3.35 \cdot 10^{14}$
0,2	50	0.1	0.8	18	∞
0,4	50	1.7	0.8	18	∞
0,6	46	87	0.8	18	∞
0,8	46	67	0.9	18	∞
PolyCoTAPP					
Potencial /V	R_s / Ω	C_{pol} / µF	C_{pol} / n	R_{pol} / kΩ	R_{ct} / Ω
0,0	37	1.2	0.9	26	∞
0,2	38	1.4	0.9	24	∞
0,4	40	1.6	0.9	31	∞
0,6	33	1.2	0.9	23	∞
0,8	34	1.2	0.9	21	∞
Poly(CoTAPP-co-*o*PD)					
Potencial /V	R_s / Ω	C_{pol} / µF	C_{pol} / n	R_{pol} / kΩ	R_{ct} / Ω
0,0	45	155	0.8	0	$3.48 \cdot 10^{5}$
0,2	46	0.4	0.7	3	∞
0,4	30	0.1	0.7	8	∞
0,6	26	0.1	0.7	10	∞
0,8	25	0.1	0.7	9	∞

For the GC/polyCoTAPP electrode there are observed almost constant values for R_s, R_p and C_{pol}, which is consistent with a voltammetric response that does not show redox processes. It acts as a porous polymer that only participates as coating.

The GC/poly(CoTAPP-co-*o*PD) electrode represents a R_{pol} at 0.0 V of 0 kΩ, a very small value if compared to the value of R_{pol} at 0.0 V (17 kΩ) for P*o*PD and at 26 kΩ for polyCoTAPP, showing a copolymer which is more conductive than its homopolymers. Besides, the value of the frequency exponent in its constant phase is of the order of 0.8 and diminishes down to 0.7 with the potential increase, indicating possible polymer degradation or dehydration, making the polymer more compact at high potentials.

On the other hand, R_{ct} values that are relatively lower at 0.0 V are obtained, because at 0.0 V the faradaic process that corresponds to the reported redox couple can be found.

If the three polymers at a given potential, at 0.2 V for example, are compared, it is obtained that the R_s are the same, thus indicating that there are no ohmic impediments. The capacity of the polymers (C_{pol}) is higher for the copolymer because it increases the amount of polymer deposited and therefore the number of active sites. The exponent of the frequency in the constant phase element (n) is lower for the copolymer that shows increase of defects or rugosity. The resistance is very high for the Co porphyrin film in respect with the polymer, because of its small growing and its is little conductivity, it is higher for the *o*PD polymer in respect to the copolymer since its more conductive than polyCoTAPP and its too small for the copolymer for a synergic effect. In this ways, it is obtained a more conductive and rugose polymer than its homopolymers according to impedance measures. This result shows also synergic effect in the copolymer conductivity if compared with both homopolymers.

3.2. Scanning Electronic Microscopy (SEM)

3.2.1. Au/polyCoTAPP, Au/PoPD and Au/poly(CoTAPP-co-oPD) electrodes SEM

SEM images show the CoTAPP and *o*PD polymers microstructure in Figure 6. Cobalt porphyrin polymer, polyCoTAPP, shows that this polymeric film (light gray dots on the Au electrode) appears on irregular shape covering very small areas. Practically, it is obtained a “clean” gold surface (see Fig.6A). On the other hand, the SEM images for the *o*PD polymer that is shown in Figure 6B show that the surface of the gold electrode (Au) is covered with a very regular rugous polymer, forming defined cracked tissue on the electrode.

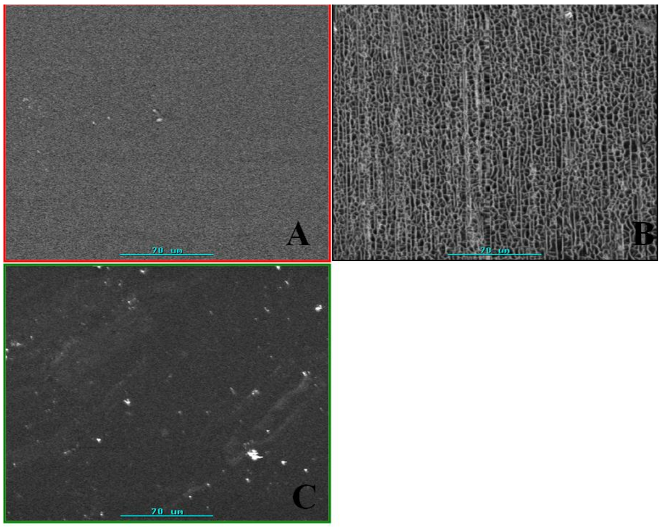

Figure 6. SEM images of Au electrode / polyCoTAPP (A), P*o*PD (B) and copolymer (C), magnification 500X.

When it is studied the Au electrode surface with the copolymer deposited in its surface (see Fig. 6C), different images compared to that presented before are obtained. In this electrode, it can be seen a rugous surface composed by the two monomers, where the cobalt porphyrin is presented in the lighter colors and the *o*PD appears like cracked tissue. It must be pointed out that in the copolymer it is observed the presence of the cobalt porphyrin in high amounts, spreading all over the mapping area, which is different to the very low amount that is observed when the cobalt porphyrin is grown without *o*PD.

It is interesting to notice that in this study also a synergic effect is obtained on the copolymer formation. When CoTAPP is electropolymerazed on the Au surface, there is practically no deposit. However, when the electropolymerization takes place simultaneously with thje polymerization *o*PD, this monomer "helps" the porphyrin to be incorporated on the surface.

3.3. Raman micro- spectroscopy

3.3.1. Au/polyCoTAPP, Au/PoPD and Au/poly(CoTAPP-co-oPD) electrodes

Figure 7 shows the Raman spectra for homo and co-polymers, and it can be observed that they are different. In the first place, it is observed a change in the intensity of the peaks ranging between 1367-1578 cm^{-1}, corresponding to the Raman region that is attributed to C=C *p*-disustituted bencene stretches, CH_2 (or NH_2) deformations at different torsion angles (1219-1458 cm^{-1}), and aromatic Schiff (C_6H_5-CH=N-R) stretches (1509-1703 cm^{-1}) [41]. Also, the spectra show displacement of 4, 5 y 9 cm^{-1} for the signals appearing at 1367, 1516 y 1578 cm^{-1} for PoPD compared to polyCoTAPP. These displacements are big enough to become new evidence supporting that the phenomenon of copolymerization between CoTAPP molecules and *o*PD molecules is truly occurring and different bonds are formed. However, the most direct evidence is obtained from the frequency change in the C-N vibration.

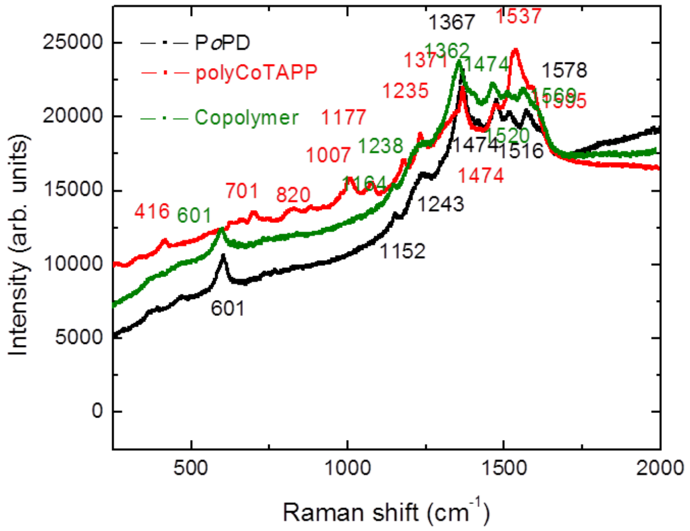

Figure 7. Raman spectra of polyCoTAPP, P*o*PD and copolymer electropolymerized on gold.

The 1516 cm^{-1} frequency in P*o*PD and 1537 cm^{-1} in polyCoTAPP which corresponds to the C-N vibration, appears for the copolymer at 1520 cm^{-1} showing that there is a C-N bound with different energy in the compolymer compared to the C-N bound of its homopolymers. Besides, there is no sight of Raman peaks for the cobalt porphyrin (416, 701, 820, 1007, 1177, 1537 and 1595 cm^{-1}, which is very crystalline in the copolymer.

It is interesting to note that the Raman spectra of the copolymer are similar to the spectrum of the P*o*PD homopolymer, although most of the signals are shifted. Practically, in the copolymer the presence of CoTAPP is not observed, but the effect of this complex on the PoPD is observed.

3.3.2 polyCoTAPP and PoPD composite electrodes

Figure 8 shows the Raman spectra obtained for the A and B composites. The A composite is formed by Au/polyCoTAPP/P*o*PD and the B composite is formed by Au/P*o*PD/polyCoTAPP. The copolymer peaks at 1164, 1238, 1474, 1520 and 1569 cm^{-1} do not appear in the A or B composite spectra. It can be observed that for the A composite the signal at 1362 cm^{-1} and for the composite B the signal at 601 cm^{-1} are the only ones that have correspondence with copolymer signals taking into consideration that the determination of a Raman signal has an error of +/- 2 cm^{-1}. Besides, the Raman signal at 1520 cm^{-1} corresponding to the C-N vibration does not appear in any of the two composites formed. Therefore, the measured copolymer spectrum showed above does not correspond to a composite, discarding this type of growing for the studied copolymer.

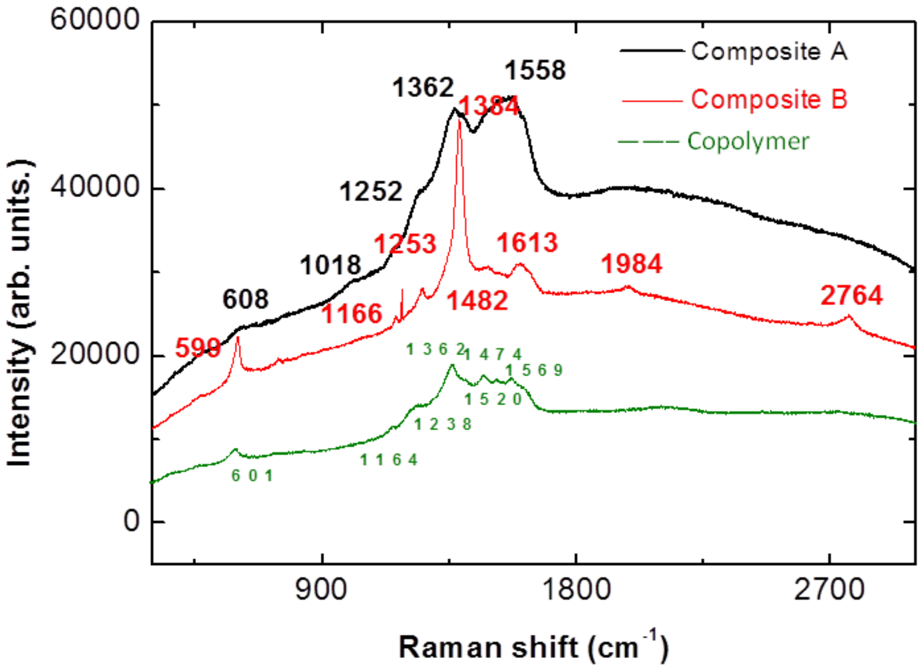

Figure 8. Comparison of Raman spectra of electropolymerized composites and copolymer on gold.

4. CONCLUSIONS

It was found a new and simple material for electrodes or poly(CoTAPP-co-*o*PD) glassy carbon modified electrodes coating. Voltammetric measurements, impedance measurements, SEM, and Raman microspectroscopy corroborate that the copolymer is electrochemically formed and it is stable and reproducible.

Besides, the poly(CoTAPP-co-*o*PD) modified electrode shows the synergy expected for the reduction of molecular oxygen in acid medium because this new material that is more conductive and rugous compared to the respective homopolymers.

ACKNOWLEDGMENTS

Financial support from Fondecyt-Regular 1100055 project and Dicyt-USACH are gratefully acknowledged. R. Arce thanks support Conicyt for PhD fellowship.

References

1. G. Kumar, A. Sivashanmugam, N. Muniyandi, S. K. Dhawan, D. C. Trivedi, *Synthetic Metals,* 80 (1996) 279.
2. M. Kurian, M. E. Galvin, P. E. Trapa, D. R. Sadoway, A. M. Mayes, *Electrochimica Acta,* 50 (2005) 2125.
3. S. Koul, R. Chandra, S. K. Dhawan, *Sensors and Actuators B,* 75 (2001) 151.
4. M. Urbanczyk, W. Jakubik, E. Maciak, A. Stolarczyk, *Molecular and Quantum Acoustics,* 25 (2004) 235.
5. S. K. Dhawan, N. Singh, D. Rodrigues, *Sci. Technol. Advanced Mater.,* 4 (2003) 105.
6. Y. Wang, X. Zing, *Polymers for Advanced Technol.,* 16 (2005) 344.
7. S. Koul, R. Chandra, S. K. Dhawan, *Polymer,* 41 (2000) 9305.
8. L. Kumar, S. K. Dhawan, M. N. Kamalsannan, S. Chandra, *Thin Solid Films,* 441 (2003) 243.
9. W. H. Kim, A. J. Makinen, N. Nikolov, N. R. Shashidhar, H. Kim, Z. H. Kafafi, *Applied Physics Letters,* 80 (2002) 3844.
10. H. Etori, J. X. Lan, T. Yasuda, S. Mataka, T. Tetsuo, *Synthetic Metals,* 156 (2006) 1090.
11. C. K. Tan, D. J. Blackwood, *Corr. Sci.,* 45 (2003) 545.
12. D. Sazou, C. Georgolios, *J. Electroanal. Chem.,* 29 (1997) 81–93.
13. W. A. Gazotti, G. Casalbore-Miceli, S. Mitzakoff, A. Geri, M. C. Gallazzi, M. A. de Paoli, *Electrochimica Acta,* 44 (1999) 1965.
14. H. H. Kyung, W. O. Kyung, K. Tae Jin, *J. Appl. Polymer Sci.,* 97 (2005) 1326–1332.
15. R. Mazeikiene, A. Malinaukas, *Synthetic Metals*, 128 (2002) 121.
16. H-P. Dai, Q-H. Wu, S-G. Sun, K-K. Shiu, *J. Electroanal. Chem.,* 456 (1998) 49.
17. K. Ogura, M. Kokura, J. Yano, H. Shigi, *Electrochimica Acta*, 40 (1995) 2707.
18. J. Yano, *Journal of Polymer Science Part A: Polymer* Chemistry, 33 (1995) 2435.
19. F. Bedioui, J. Devynck. *Accounts of Chemical Research,* 28, (1996) 30.
20. M. Biesaga, K. Pyrzynska, M. Trojanowicz, *Talanta,* 51 (2000) 209.
21. N. S. Trofimova, A. Y. Safronov, O. Ikeda, *Electrochimica Acta*, 50 (2005) 4637.
22. J. Manríquez, J. L. Bravo, S. G. Granados, S. S. Succar, C. Bied Charreton, A. A. Ordaz, F. Bedioui, *Analytica Chimica Acta*, 378 (1999) 159.
23. D. Mimica, J. H. Zagal, F. Bedioui, *Electrochem. Commun.*, 3 (2001) 435.
24. K. I. Ozoemena, T. Nyokong, *Talanta*, 67 (2005) 162.
25. K. I. Ozoemena, Z. Zhao, T. Nyokong, *Electrochem. Commun.*, 7 (2005) 679.

26. A. Camargo, M. J. Aguirre, W. Cheuquepán, Y. Chen, G. Ramírez, *Electroanalysis* 20 (2008) 2635.
27. F. Armijo, M. Isaacs, G. Ramírez, E. Trollund, J. Canales, M.J. Aguirre, *J. Electroanal. Chem.*, 566 (2004) 315.
28. M. Lucero, G. Ramírez, A. Riquelme, I. Azocar, M. Isaacs, F. Armijo, J.E. Förster, E. Trollund, M. J. Aguirre, D. Lexa, *Journal of Molecular Catalysis A: Chemical*, 221 (2004) 71.
29. R. Ríos, A. Marín, G. Ramírez, *J. Coordination Chem.*, 63 (2010) 1284.
30. M. Lucero, M. Riquelme, G. Ramírez, M. C. Goya, A. González Orive, A. Hernández Creus, M. C. Arévalo, M. J. Aguirre, *Int. J. Electrochem. Sci.*, 7 (2012) 234-250.
31. G. Cornejo, G. Ramírez, M. Villagrán, J. Costmagna, E. Trollund, M. J. Aguirre, *Boletín de la Sociedad Chilena de Química*, 485 (2003) 49.
32. S-M. Chen, Y-L. Chen, *J. Electroanal. Chem.*, 573 (2004) 277.
33. H. Bhandari, V. Choudhary, S. K. Dhawan, *Polymer Adv. Technol.*, 20 (2009) 1025.
34. M. Lucero, M. Riquelme, G. Ramírez, M. C. Goya, A. González Orive, A. Hernández Creus, M. C. Arévalo, M. J. Aguirre, *Int. J. Electrochem. Sci.*, 7 (2012) 236.
35. L. Ugalde, J. C. Bernede, M. A. del Valle, F. R. Díaz, P. Leray, *J. Appl. Polymer Sci.*, 84 (2002) 1799-1809.
36. M. A. del Valle, L. Ugalde, F. R. Díaz, M. E. Bodini, J. C. Bernede, *J. Appl. Polymer Sci.*, 92 (2004) 1346-1354.
37. M. A. del Valle, M. B. Camarada, F. Díaz, G. East, *e-Polymers*, (2008) no. 072.
38. S. Griveau, V. Albin, T. Pauporté, F. Bedioui, J. H. Zagal, *J. Mater. Chem.*, 12 (2002) 225-232.
39. M. A. del Valle, F. R. Díaz, M. E. Bodini, G. Alfonso, G. M. Soto, E. D. Borrego, *Polymer Int.*, 54(3) (2005) 526–532.
40. L. L. Wu, J. Luo, Z. H. Lin, *J. Electroanal. Chem.*, 417(1-2) (1996) 53.
41. X-G. Li, M-R. Huang, R-F. Chen, Y. Jin, Y-L. Yang, *J. Polymer Sci. A Polym. Chem.* 39(22) (2001) 3989.
42. X. Sun, M. Hagner, *Langmuir* 23(21) (2007) 10441.
43. S. R. Sivakkumar, R. Saraswathi, *J. Appl. Electrochem.*, 34 (2004) 1148.
44. K. Martinusz, G. Láng, G. Inzelt, *J. Electroanal. Chem.*, 433 (1997) 4.
45. D. I. Bower, W. F. Maddams, *The characterization of polymers.* Cambridge: Editorial Cambridge University Press, (1989).